Molecular Therapy
Original Article

Hypoxic Lung-Cancer-Derived Extracellular Vesicle MicroRNA-103a Increases the Oncogenic Effects of Macrophages by Targeting PTEN

Ya-Ling Hsu,[1] Jen-Yu Hung,[2,3] Wei-An Chang,[2,4] Shu-Fang Jian,[4] Yi-Shiuan Lin,[4] Yi-Chung Pan,[4] Cheng-Ying Wu,[4] and Po-Lin Kuo[1,4,5]

[1]Graduate Institute of Medicine, College of Medicine, Kaohsiung Medical University, Kaohsiung 807, Taiwan; [2]Division of Pulmonary and Critical Care Medicine, Kaohsiung Medical University Hospital, Kaohsiung 807, Taiwan; [3]School of Medicine, College of Medicine, Kaohsiung Medical University, Kaohsiung 807, Taiwan; [4]Graduate Institute of Clinical Medicine, College of Medicine, Kaohsiung Medical University, Kaohsiung 807, Taiwan; [5]Institute of Medical Science and Technology, National Sun Yat-Sen University, Kaohsiung 804, Taiwan

Hypoxia, the most commonly observed characteristic in cancers, is implicated in the establishment of an immunosuppressive niche. Recent studies have indicated that extracellular vesicle (EV)-mediated cancer-stroma interactions are considered to play a critical role in the regulation of various cellular biological functions, with phenotypic consequences in recipient cells. However, the mechanisms underlying the relationship between EVs and hypoxia during cancer progression remain largely unknown. In this study, we found that EVs derived from hypoxic lung cancers increased M2-type polarization by miR-103a transfer. Decreased PTEN levels caused by hypoxic cancer-cell-derived EV miR-103a increased activation of AKT and STAT3 as well as expression of several immunosuppressive and pro-angiogeneic factors. In contrast, inhibition of miR-103a by an miRNA inhibitor effectively decreased hypoxic cancer-mediated M2-type polarization, improving the cytokine prolife of tumor infiltration macrophages. Macrophages received cancer-cell-derived EV miR-103a feedback to further enhance cancer progression and tumor angiogenesis. Finally, circulating EV miR-103a levels were higher in patients with lung cancer and closely associated with the M2 polarization. In conclusion, our results delineate a novel mechanism by which lung cancer cells induce immunosuppressive and pro-tumoral macrophages through EVs and inspire further research into the clinical application of EV inhibition or PTEN restoration for immunotherapy.

INTRODUCTION

There were an approximately 1.8 million newly diagnosed cases of lung cancer globally in 2012, and the number is expected to rise to 24 million by 2035. Over 1.6 million people are expected to die from lung cancer, accounting for more than 20% of all cancer deaths, making it to the most lethal malignancy worldwide.[1,2] The 5-year survival rate for lung cancer is less than 15%, and although there has been some improvement in lung cancer outcomes over the past few decades, the prognosis for lung cancer is still poor in comparison with other common malignancies.[3] Work in understanding lung cancer biology continues to be important.

The tumor microenvironment (TME) has been shown to play a pivotal role in all stages of cancer development: immunosuppression, tumorigenesis, cancer growth, progression, angiogenesis, and metastasis, through secreted factors, cell-cell interactions, and matrix remodeling.[4,5] Tumor-associated macrophages (TAM) represent a prominent immune population in TME and are associated with poor prognosis in patients with malignant tumors.[6,7] In most types of cancer, monocytes are recruited from the circulation and differentiated to TAMs under the influence of the TME. Macrophages are classified into two subpopulations: the classic M1 and the alternative M2 macrophages.[8] Classically activated macrophages (M1 macrophages), driven by the Th1 cytokine interferon (IFN)-γ, express pro-inflammatory factors such as interleukin-6 (IL-6), IL-12, and IL-23 and are potent executive cells that destroy cancer cells. Conversely, alternatively activated macrophages (M2 macrophages), upregulate the expression of macrophage mannose receptors (CD206), scavenger receptors, and CD163, as well as M2-type immunosuppressive cytokines (IL-10).[9,10] TAM, driven by the TME, exerts an M2 phenotype, which loses cytotoxic ability and, instead, exhibits various pro-tumoral activities, including cancer-related inflammation, immunosuppression, angiogenesis, tissue remodeling, and metastasis.[11–13] TAMs emerge as prospective targets for innovative therapeutic strategies aimed at reprogramming their pro-tumoral phenotype toward an effective anticancer activity.[8] However, some studies indicate that the diversity of the macrophage infiltration in cancer potentially may have both protumoral and antitumoral functions.[14,15] Macrophages phenotypically adapt to suit the

Received 15 May 2017; accepted 25 November 2017;
https://doi.org/10.1016/j.ymthe.2017.11.016.

Correspondence: Po-Lin Kuo, Graduate Institute of Clinical Medicine, College of Medicine, Kaohsiung Medical University, No. 100, Shih-Chuan 1st Road, Kaohsiung 807, Taiwan.
E-mail: kuopolin@seed.net.tw

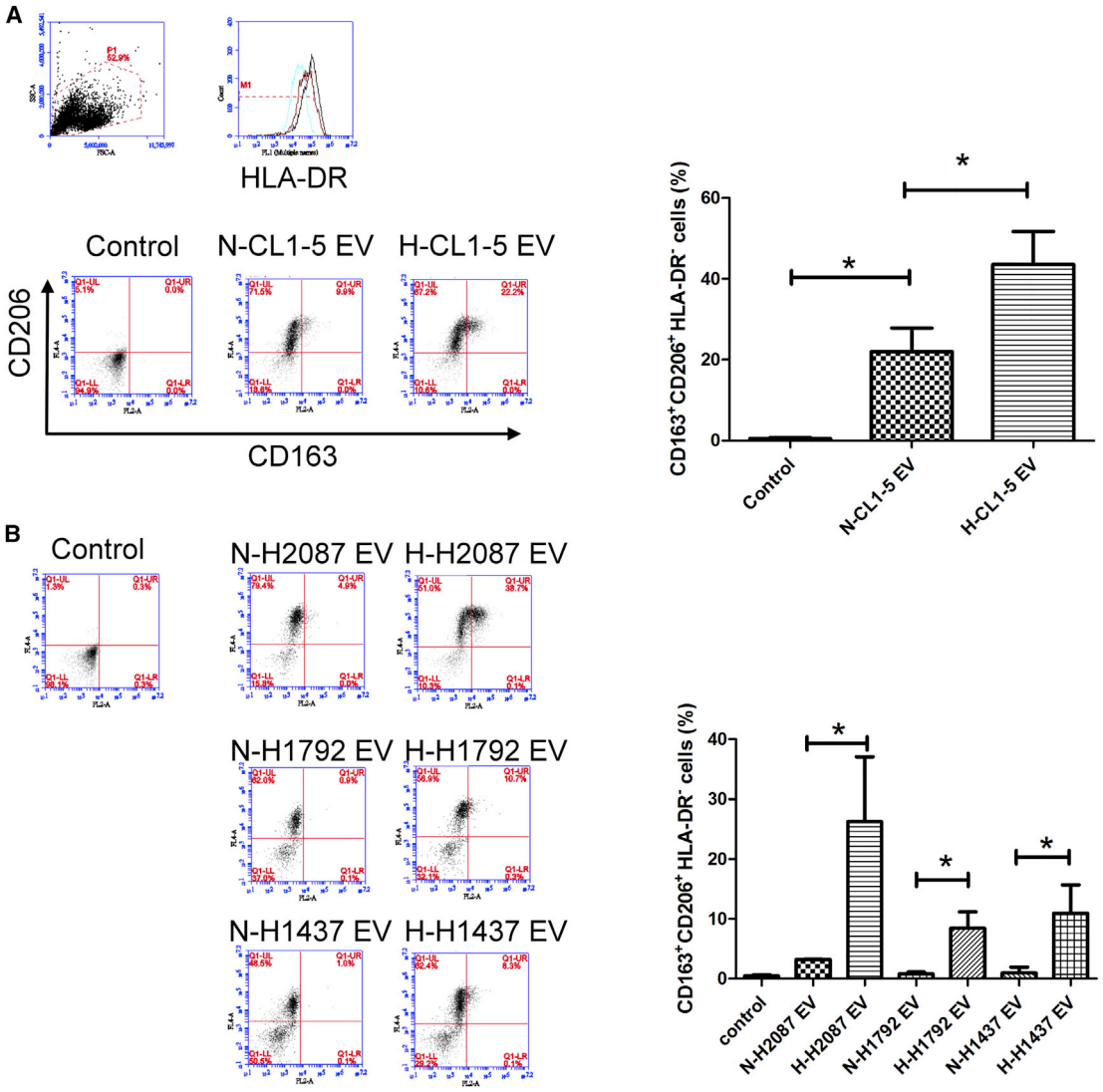

Figure 1. Hypoxic Lung-Cancer-Secreted EVs Increases M2 Polarization

(A) Flow cytometry analysis reveals that EV isolated hypoxic lung cancer CL1-5 cells increase the population of $CD163^{+}CD206^{high}HLA\text{-}DR^{low}$ cells. Live cells (p1) were selected on the basis of forward scatter pulse area (FSC-A) and side scatter pulse area (SSC-A). $HLA\text{-}DR^{low}$ (M1) cells gated as $CD163^{+}CD206^{high}$ were analyzed as dot plots showing double fluorescence on gated $HLA\text{-}DR^{low}$ live cells (M1). (B) EVs isolated from three hypoxic lung cancer cell lines also enhanced M2 polarization. $CD14^{+}$ monocytes were treated with EVs isolated from normoxic (20% oxygen, 24-hr culture) and hypoxic (1% oxygen, 24-hr culture) lung cancer cells containing M-CSF (20 ng/mL) for 5 days. The expressions of various surface markers were stained and assessed by flow cytometry. Data are expressed as mean ± SD. *$p < 0.05$. All experiments were performed independently at least 3 times. EV, extracellular vesicles; N-, normaxia; H-, hypoxia.

microenvironment in response to various stimuli and cytokines. TAMs exhibit anti-tumor immunity and reduce angiogenesis in normoxic regions, while they escape antitumor immunity and promote vascularization in hypoxic niches.[16] This requires an in-depth understanding of the molecular mechanisms for macrophages' subset switches, as well as the dynamic interaction between cancer-macrophages in TME.

A growing body of studies have shown that in addition to initiation via soluble mediators, cell-cell communication can be initiated through circulating extracellular vesicles (EVs).[17,18] The transfer of microRNA (miRNA) by EVs is especially interesting, since miRNAs could regulate the levels of multiple target genes in the recipient cells if they engulf EVs secreted from local or distant sites in the body.[19] Hypoxia is considered to be the primary culprit that shapes TME and causes cancer growth and progression.[20,21] Emerging evidence suggests a strong link between tumor hypoxia and immune suppression.[22,23] In a previous study, we demonstrated that hypoxia increased lung cancers' secretion of EVs, which consequently enhanced tumor angiogenesis and blood vessel permeability, resulting in increased

Table 1. Hypoxic Lung-Cancer-Secreted Exosomes Increase the Expression of M2-type Cytokines and Proangiogenic Factors

		CL1-5	
Control (Mock)		Normoxia	Hypoxia
Cytokines (pg/mL)			
IL-12	0.79 ± 0.33	1.52 ± 0.57	1.90 ± 0.69
IL-10	543.72 ± 129.07	1,308.39 ± 387.51	2,305.31* ± 1,035.48
CCL18	814.68 ± 557.36	823.92 ± 356.27	1,226.27* ± 223.45
CCL22	1,682.81 ± 680.08	926.90 ± 265.96	2391.82 ± 501.82
TNF-α	582.89 ± 284.8	638.28 ± 249.10	878.62* ± 123.81
Proangiogenic Factors (pg/mL)			
VEGF-A	156.88 ± 95.35	446.32 ± 154.59	1,320.13* ± 663.90
Angiopoietin-1	503.30 ± 280.64	644.18 ± 123.27	798.97* ± 115.75
Angiogenin	3,854.78 ± 871.01	3,075.84 ± 415.49	5,509.74* ± 708.34
FGF basic	20.712 ± 4.12	18.62 ± 3.79	18.91 ± 3.72
FGF acidic	7.16 ± 1.50	11.62 ± 4.37	10.74 ± 3.05
PDGF-AA	46.53 ± 11.59	52.04 ± 16.04	48.22 ± 10.53
PDGF-BB	614.19 ± 225.85	527.63 ± 294.69	494.65 ± 362.31
PIGF	1.41 ± 0.24	1.79 ± 0.30	1.79 ± 0.29
VEGF-D	16.97 ± 2.63	20.74 ± 6.53	20.05 ± 6.21

*$p < 0.05$ versus Normoxica. FGF, fibroblast growth factor.

metastasis. In the present study, we investigate the role of lung-cancer-derived EVs in the reprogramming of macrophages in hypoxic TME. We conclude that hypoxia induces lung cancer to alter the macrophage phenotype toward pro-tumoral activity through EVs-mediated delivery of oncogenic miR-103a. Our study provides new insight into understanding the unique crosstalk that accounts for an immunomodulatory pheromone in hypoxic TME.

RESULTS

Hypoxic Lung-Cancer-Secreted EVs Increase M2 Macrophage Polarization *Ex Vivo*

To investigate whether hypoxic lung cancer alters differentiation and function of macrophages, we assessed the immune-phenotype and cytokine profile of macrophages that were differentiated from $CD14^+$ monocytes presented with EVs isolated from CL1-5 lung cancer cells under normoxic and hypoxic conditions. EVs isolated from normoxic CL-15 cancer cells increased the population of M2 phenotype macrophages ($CD163^+CD206^{high}HLA\text{-}DR^{low}$). EVs derived from hypoxic CL1-5 cells further increased the population of M2 macrophages (Figure 1A). Consistent with the changes in surface markers, macrophages treated with EVs from hypoxic CL-15 cancer cells produced significantly more M2-type (IL-10, chemokine [C-C motif] ligand [CCL18], and CCL22) and tumor-promoting cytokines (tumor necrosis factor alpha [TNF-α], vascular endothelial growth factor A [VEGF-A], and angiopoietin-1) than did untreated macrophages or those treated with EVs from normoxic CL1-5 cancer cells (Table 1). Depletion of EVs by microfilter decreased the effect of hypoxic CL1-5-derived EVs in M2 polarization and M2-type cytokine (IL-10, CCL18, and CCL22) production (Figures S1A–S1D), suggesting that hypoxic CL1-5-derived EVs contribute to the induction of M2 polarization caused by hypoxic lung cancer. Moreover, EVs isolated from three hypoxic lung cancer cell lines (NCI-H2087, -H1792, and -H1437) also changed their surface markers and M2 cytokines, as well as tumor-promoting factors, more than those macrophages treated with EVs from normoxic lung cancer cell lines (Figure 1B; Table S1).

Hypoxic Lung-Cancer-Secreted EVs Altered Macrophage Phenotype via EV miR-103a

Previous data show that hypoxia stimulates the secretion of EV miR-103a in lung cancers.[24] Therefore, we assessed the possible role of miR-103a in lung-cancer-mediated M2 macrophage polarization under hypoxic conditions. Since hypoxia stimulates CL1-5 cells to produce EVs,[24] we measured levels of miR-103a in equal weight of EVs in normoxic and hypoxic CL1-5 cells to further clarify the upregulation of miR-103a in hypoxic CL1-5-derived EVs. The results show that levels of miR-103a in hypoxic CL1-5-secreted EVs was higher than that of normoxic CL1-5-secreted EVs (Figure S2A). We confirmed that hypoxic CL1-5-secreted miR-103a can be transferred to $CD14^+$ monocytes by EVs and then measured the miR-103a levels in monocytes treated with EVs derived from CL1-5 cells under normoxic and hypoxic conditions. An elevation of the cellular level of mature miR-103a in an EV dose-dependent manner, but not pri- or pre-miR-103a, was observed in recipient monocytes after treatment with hypoxic CL1-5-derived EVs (Figure 2A). Similarly, pri- or pre-miR-103a was also no significantly difference in the normoxic or hypoxic CL1-5-derived EVs (Figure S2B). In treatment of $CD14^+$ monocytes with EVs released from hypoxic CL1-5 cells transfected with Cy3-labeled miR-103a, Cy3 fluorescence was observed in the recipient monocytes (Figure 2B). RNA polymerase II inhibitor did not affect the increase of miR-103a in recipient monocytes, showing that enhancement of cellular miR-103a in monocytes arose from EV-mediated miRNA transfer, but not endogenous miR-103 induction (Figure 2C). The biologic function of EV miR-103a on M2 macrophage polarization was also confirmed by miR-103a inhibitor transfection in recipient monocytes. As shown in Figure 2D, the effect of hypoxic CL1-5 EVs on M2 macrophage polarization, M2 cytokines (IL-10 and CCL18), as well as VEGF-A expression, was prevented by transfecting the recipient monocytes with miR-103a inhibitor (Figures 2E–2G). In addition, levels of miR-103a in CL1-5 and NCI-H2087 were higher than those in NCI-H1792 ≈ NCI-H1437 cells, which correlates with the potency of M2 polarization caused by these lung cancer cell lines (CL1-5 ≈ NCI-H2087 > NCI-H1792 ≈ NCI-H1437) (Figures 1 and S2C).

The regulation of miR-103a on the polarization of macrophages was also validated using miR-103a mimic transfection. As shown in Figure 3A, $CD14^+$ monocytes transfected with miR-103a mimics enhanced the population of a $CD163^+CD206^{high}HLA\text{-}DR^{low}$ phenotype of macrophages after a 5-day differentiation, compared to those cells transfected with control mimics. Consistent with the alterations in phenotype, macrophages transfected with miR-103a mimics

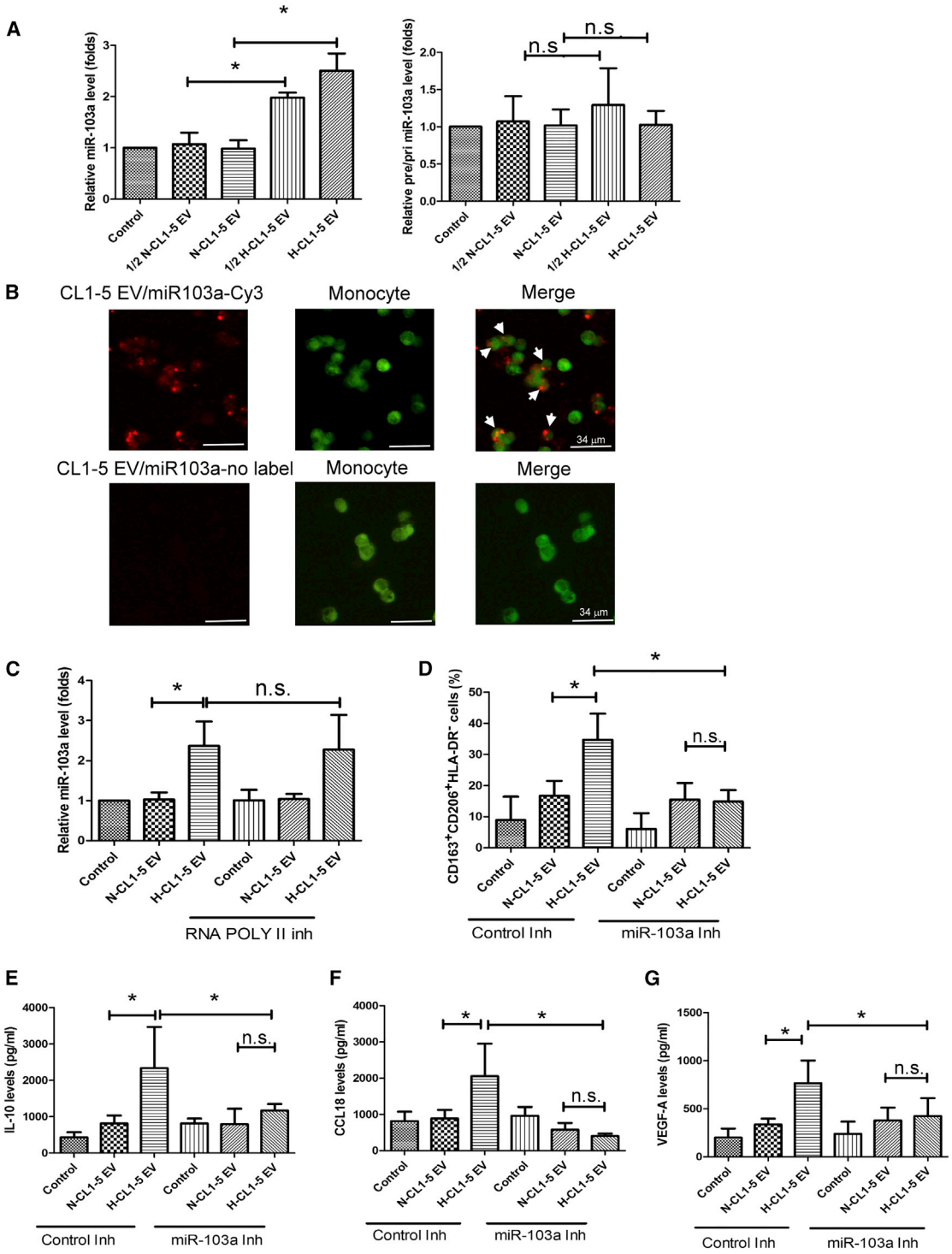

Figure 2. Hypoxic Lung Cancer Cells Increase M2 Polarization by EV miR-103a Transfer

(A) The level of pre/pri-miR-103a and mature miR-103a in $CD14^+$ monocytes receiving EVs after a 12-hr treatment. $CD14^+$ monocytes were treated with either normoxic or hypoxic CL1-5-derived EVs (monocyte/lung cancer 1:5 (label as 1/2 EVs) or 1:10 (label as EVs), and the level of pre/pri- and mature miR-103a was assessed by quantitative real-time PCR. (B) The uptake of hypoxic lung-cancer-secreted EVs in $CD14^+$ monocytes. The EVs of naked miR-103a or Cy3-labeled miR-103a-transfected CL1-5 were collected and then added to $CD14^+$ monocytes, with the uptake of EVs made visible using a fluorescence microscope. The arrows indicate the CD14 monocytes uptake EVs. (C) RNA polymerase II inhibitor did not affect the increase of miR-103a in recipient monocytes. $CD14^+$ monocytes were treated with polymerase II

(legend continued on next page)

produced significantly more IL-10, CCL18, and VEGF-A than those transfected with control mimics (Figures 3B–3D).

EV miR-103a Changes Macrophages by Targeting PTEN

We performed experiments to determine possible miR-103a targets that may contribute to its regulation activity in macrophage polarization by using three predicted miRNAs websites, including Targetscan, MiRanda, and Pictar. *In silico* analysis predicted a single, species-conserved miR-103a binding site in the 3′ UTRs of PTEN (Figures 4A and S3A), which has been reported to regulate macrophage polarization.[25] 3′ UTR luciferase reporter analysis has shown that hypoxic CL1-5-derived EV miR-103a and miR-103a mimics exhibit a direct binding on the wild-type 3′ UTR of PTEN, but not on mutated 3′ UTR luciferase plasmid (Figures 4B and 4C). Consistent with the 3′ UTR luciferase reporter analysis, hypoxic CL1-5-derived EV miR-103a and miR-103a mimics decreased the expression of PTEN (Figures 4D and S3B).

The role of PTEN in macrophage polarization and cytokine production was assessed using PTEN small interfering RNA (siRNA) transfection. $CD14^+$ monocytes transfected with PTEN siRNA, which reduced expression of PTEN by approximately 60% (Figure S4A), exhibited a $CD163^+CD206^{high}HLA\text{-}DR^{low}$ phenotype, compared to control siRNA transfection (Figure S4B). Consistent with the changes in the M2 phenotype, macrophages transfected with PTEN siRNA produced significantly higher levels of IL-10, CCL18, and VEGF-A than those cells transfected with control siRNA (Figures S4C–S4E). Moreover, the effects of hypoxic CL1-5-derived EVs on M2 phenotype polarization were also abolished by ectopic expression of PTEN (Figures 4E and 4F).

PI3K/AKT and STAT3 Axis Contributes to EV miR-103a-Mediated M2 Macrophage Polarization

Previous studies have indicated that PTEN regulates macrophage differentiation and function via both PI3K/AKT and STAT3 pathways.[26] We sought to determine whether EV miR-103a was dependent on PI3K activation by using PI3K inhibitors. As shown in Figures S3B and 5A, hypoxic CL1-5-derived EVs and miR-103a mimics transfection not only increased the phosphorylation of AKT, but also enhanced the phosphorylation of STAT3. However, they did not alter the activation of STAT6. Inhibition of PI3K by a specific chemical inhibitor (LY29004, 1 μM) prevented the M2 polarization induced by miR-103a mimics and hypoxic CL1-5-derived EVs (Figures 5B and 5C). In addition, PI3K inhibitor also decreased the upregulation of miR-103a mimics and hypoxic CL1-5-derived EVs in M2 cytokines (IL-10 and CCL18) and VEGF-A expression (Figures 5D–5I). Moreover, STAT3 inhibitors also decreased the upregulation of miR-103a mimics and hypoxic CL1-5-derived EVs in M2 cytokines (IL-10 and CCL18) and VEGF-A expression (Figures 5B–5I). These data suggest that PI3K/AKT and STAT3 are the major regulators in M2 polarization induced by hypoxic lung cancer cells via EV-mediated cancer-cell-macrophage-interaction.

EV miR-103a Increases the Stimulatory Effects of Macrophages on Cancer Progression and Angiogenesis

TAM is widely known to be involved in all stages of cancer progression, including angiogenesis, cancer cell motility, invasion, intravasation and extravasation at the metastatic site.[27] We sought to determine whether the promotive effect of macrophages in cancer progression and angiogenesis is derived from hypoxic lung cancer-secreted EV miR-103a. We therefore collected the CMs of macrophages that were treated with either CL1-5-derived EVs or transfected with miR-103a mimics. As shown in Figures 6A–6D, the CMs of hypoxic CL1-5-derived EVs treated or miR-103a mimic transfected macrophages increased CL1-5 migration and invasion, compared to CMs obtained from normoxic CL1-5-derived EVs treated or control mimic transfected macrophages. In addition, CMs of hypoxic CL1-5-derived EVs treated or miR-103a mimic transfected macrophages also enhance angiogenesis (Figures 6E and 6F). These data are consistent with results that show hypoxic CL1-5-derived EVs or miR-103a mimics increased the expression of angiogenic factors VEGF-A and angiopoietin-1 (Figure 3D; Table 1).

Higher Levels of EV miR-103a Increase M2 Macrophage Polarization and Proangiogenic Factor Expression

Next, we determined whether levels of circulating EV miR-103a are increased in patients with lung cancer. As shown in Figure 7A, EV miR-103a levels were significantly higher in patients with lung cancer (n = 24) compared to those in healthy donors (n = 25). To further determine if circulating miR-103a in patients with lung cancer is functionally active in M2 polarization, we treated $CD14^+$ monocytes with EVs isolated from the sera of healthy donors and patients with lung cancer. The results show that EVs isolated from patients with lung cancer increased M2 polarization (Figure 7B). Consistent with the changes in surface markers, macrophages treated with EVs isolated from the sera of patients with lung cancer produced significantly more M2-type cytokines (IL-10) and tumor-promoting cytokines (VEGF-A) than those treated with EVs isolated from healthy donors (Figures 7C–7E). Moreover, the promotive effect of EVs on M2 polarization, IL-10 expression, and VEGF-A expression was positively correlated with miR-103a levels (Figures 7F–7H). Our results convincingly prove that high levels of circulating miR-103a effectively increase M2 polarization among patients with lung cancer.

inhibitors (5,6-dichloro-1-β-D-ribofuranosylbenzimidazole, 20 μM) for 3 hr and then incubated with either normoxic or hypoxic CL1-5-derived EVs. Levels of mature miR-103a were assessed by quantitative real-time PCR. (D–G) Transfection of monocytes with miR-103a inhibitors prevents the effect of hypoxic CL1-5-derived EVs on the increase of M2 polarization (D), IL-10 expression (E), CCL18 (F) expression, and VEGF-A production (G). $CD14^+$ monocytes were transfected with miR-103a inhibitor for 24 hr and then incubated with either normoxic or hypoxic CL1-5-derived EVs for another 5 days. The expression of surface markers was assessed by flow cytometry; the expression of secreted proteins was determined by the Luminex system. Data are expressed as mean ± SD. *$p < 0.05$; ns, not significant. All experiments were performed independently at least 3 times. RNA POLY II inh., RNA polymerase II inhibitors. Scale bar, 34 μm.

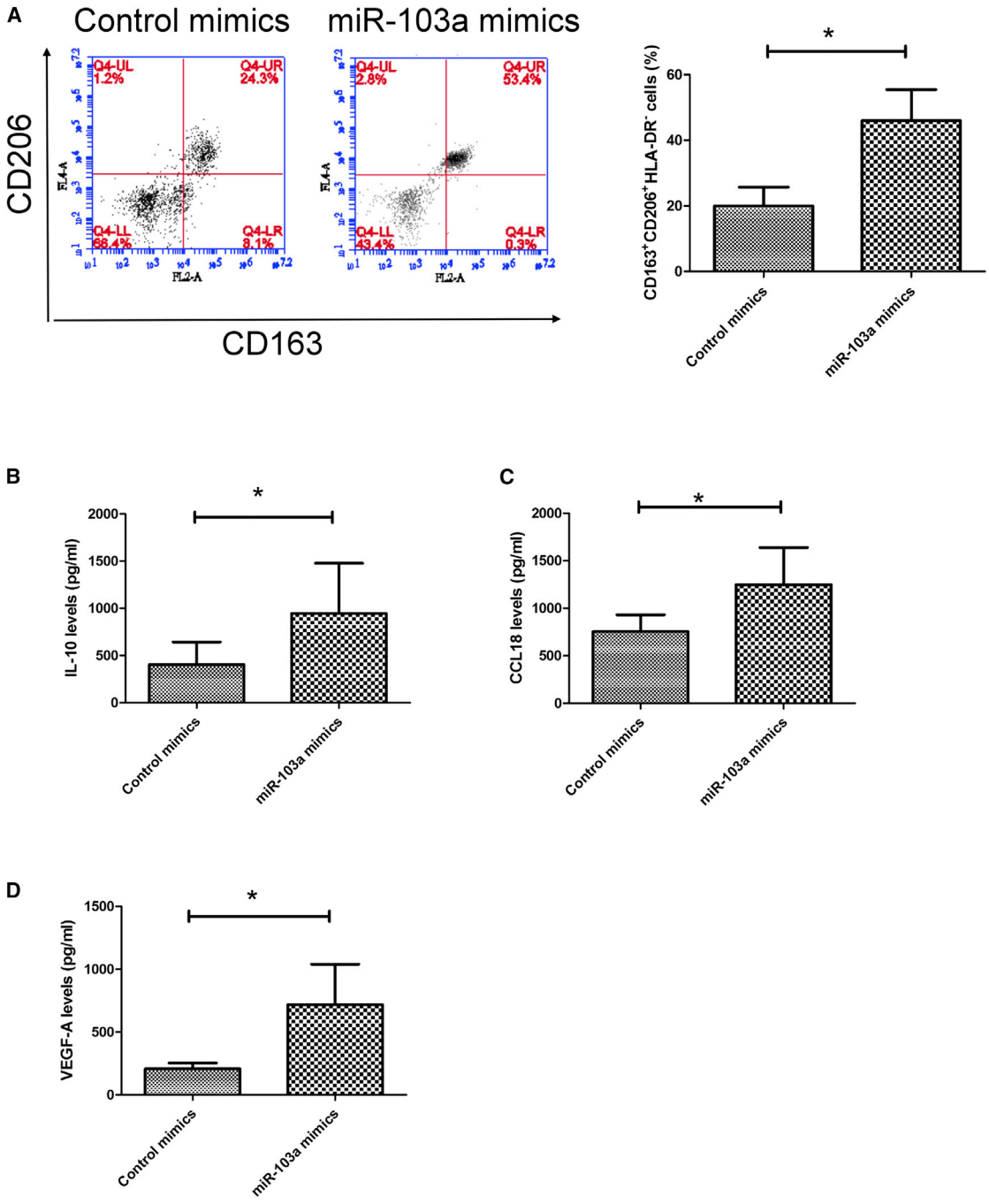

Figure 3. miR-103a Mimics Increase M2 Polarization and M2-type Cytokine Expression

(A) Flow cytometry analysis reveals that transfection of miR-103a mimics increases the population of $CD163^{+}CD206^{high}HLA\text{-}DR^{low}$ cells. (B–D) The effects of miR-103a mimics on the expression of IL-10 (B), CCL18 (C), and VEGF-A (D). $CD14^{+}$ monocytes were transfected with either control or miR-103a mimics and then cultured for another 5 days. The expression of surface markers was assessed by flow cytometry, and the expression of secreting proteins was determined by the Luminex system. Data are expressed as mean ± SD. *$p < 0.05$ versus control mimics. All experiments were performed independently at least 3 times.

DISCUSSION

Hypoxia has been demonstrated to be the major driving force for TME remodeling that promotes cancer progression and chemoresistance.[28] The bidirectional communication in TME that occurs between lung cancer and immune cells not only effectively remodels immune cells to an immune-suppressing phenotype that allows

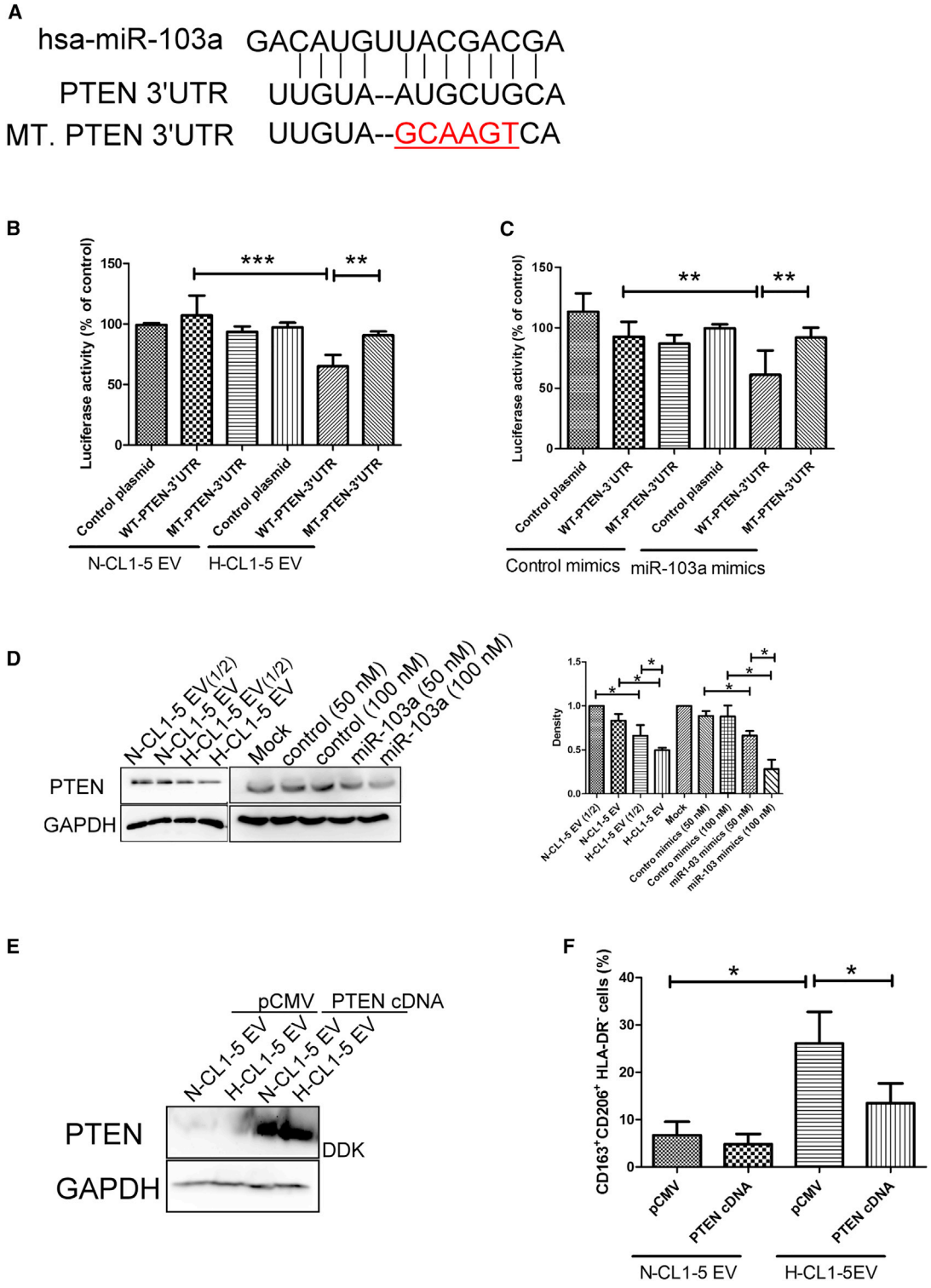

Figure 4. PTEN Is the Target of EV miR-103a

(A–F) The schematic representation of the pGL3 luciferase reporter construct containing the PTEN-1 3′ UTR region cloned downstream of the firefly luciferase gene. (A) The diagrams of the wild-type luciferase plasmid containing miR-103a binding site in this region (3′ UTR WT) and its mutated form (3′ UTR MT) are shown. (B and C) The binding activity of hypoxic CL1-5-derived EVs 103a (B) and miR-103a mimics (C) in the 3′ UTR of PTEN, as determined by a 3′ UTR luciferase report analysis. HEK293 cells were

(legend continued on next page)

cancer to develop, but also confers an optimal TME for the cancer cells to progress and metastasize.[21] A growing number of studies have shown that cancer cells and immune cells can interact via the exchange of bioactive molecules through extracellular vesicles, resulting in the exchange of genetic material over a distance.[29,30] Our previous study indicates that hypoxia stimulates lung cancer to release extracellular vesicles, which contain significantly higher levels of miRNAs, including miR-103a, -23a, -370, and -373. Of these, miR-23a contributes to the increase of tumor angiogenesis and vascular permeability by targeting prolyl hydroxylase and tight junction protein ZO-1 in both normoxia and hypoxia TME.[24] In this study, we showed that EVs miR-103 can be transferred from hypoxic cancer cells to macrophages, resulting in the enhancement of M2 polarization by the downregulation of miR-103a's direct target PTEN (Figure 7I). Our series of studies shows that EVs play a critical role in the shape of TME driven hypoxia.

EV-delivery cell-cell communication is considered to be an effective mode to regulate cell signaling and biological behaviors in recipient cells. Thus, EVs play a critical role in the establishment of TME through the interplay between tumor cells and normal cells, thereby facilitating cancer development.[31] miR-103 has been found to be upregulated in numerous cancers, including endometrial cancer, nasopharyngeal carcinoma, pancreatic cancer, bladder cancer, colorectal cancer and lung cancer.[32] Previous studies have reported that miR-103 promotes tumor growth and metastasis in cancers by directly targeting AKAP12/Gravin[33] and LATS2.[34] miR-103 has also been found in exosomes isolated from cerebrospinal fluid of patients with glioblastoma.[35] miR-103a is a hypoxia-responsive miRNA, thus is considered to be involved in the reprogrammed function of hypoxia in TME, including angiogenesis and immune editing.[36] In this study, we determined that hypoxia stimulates lung cancer to secrete EVs containing miR-103a, which in turn is successfully transferred to monocytes, polarizing them toward immunosuppressive M2-type macrophages. Depletion of EVs reduces the activity of hypoxic lung cancer in M2 polarization. In addition, EV miR-103a-derived macrophages express high levels of tumor promotive and proangiogenic factors VEGF and angiopoietin-1, which increases cancer migration, invasion and angiogenesis. Moreover, significantly higher EV miR-103a levels are detected in the sera of patients with lung cancer. Understanding the mechanisms and then relevance to hypoxia and M2-type polarization will offer further incentives for targeting miR-103a as a strategy toward subverting TME for a favorable anti-cancer impact.

PTEN is a known tumor suppressor that is frequently inactivated in a variety of human cancers, including lung cancer.[37] An increasing number of studies have demonstrated that genetic inactivation of PTEN contributes to the initiation, progression and malignant transformation of cancers.[38,39] PTEN has been implicated in immunity modulation by regulating the PI3K/AKT axis signaling pathway, and its inactivation or deficiency facilitates M2-type polarization and dampens the expression of proinflammatory cytokines.[27,40,41] Inhibition of PTEN increases the activation of AKT and STAT3, which in turn enhances the accumulation of $CD163^{+}CD206^{high}HLA\text{-}DR^{low}$ cells and expression of cancer-promoting factors, including IL-10, CCL-2 and VEGF-A.[22,23] Here, we have identified miR-103a as a key regulator of PTEN, suggesting that it is one mechanism associated with M2 macrophage polarization. Our results show that hypoxic lung cancer cells decrease PTEN levels in the monocytes of tumor microenvironments by secreting EV miR-103a, and then increasing M2 macrophage polarization. The absence of PTEN in hypoxic lung cancer-derived EV miR-103a is associated with the overactivation of AKT and STAT3. Inhibition of PI3K decreases the expression of IL-10, CCL18 and VEGF-A in macrophages which receive EV miR-103a secreted by hypoxic lung cancer cells. The pro-tumorigenic activities of cancer EV-derived macrophages are also supported by the CMs of macrophage increased cancer migration and angiogenesis after receiving hypoxic cancer cell-producing EVs. Therefore, we conclude that tumor hypoxia switches macrophages from tumor-suppressing to tumor-promoting by secreting EV miR-103a, which directly targets PTEN and causes activation of PI3K/Akt and STAT3 signaling pathways.

In conclusion, we have demonstrated that EV miR-103a confers immunosuppressive and tumor-promotive phenotypes on macrophages through its transfer from hypoxic cancer cells to monocytes. Furthermore, we suggest that preventing the EV transfer from hypoxic cancer cells or miR-103a inhibition is a novel adjuvant to activate immune responses against lung cancer. In addition, the identification of PTEN as a direct target of miR-103a is obligatory for determining M2 polarization, suggesting that strategies based on the upregulation of PTEN in lung cancer can be used to improve macrophage-mediated promotion of malignancy.

MATERIALS AND METHODS

Cell Lines

Human adenocarcinoma cell lines NCI-H1437, NCI-H1792, and NCI-H2087 and human embryonic kidney HEK293 cells were purchased from American Type Culture Collection (Manassas, VA, USA), and the CL1-5 cells were kindly provided by Dr. Pan-Chyr Yang of National Taiwan University. NCI-H1437, NCI–H1792, NCI-H2087, and CL1-5 cells were maintained at 37°C, in a 5% CO_2 humidified atmosphere, in complete RPMI1640 medium

co-transfected with miR-103a with 3′ UTR luciferase/renilla plasmid (10:1). Luciferase activity was measured 48 hr after transfection using the dual luciferase reporter assay system. Firefly luciferase activity was normalized to renilla luciferase activity for transfection efficacy. (D) miR-103a and hypoxic CL1-5-derived EV miR-103a decreased the expression of PTEN in HEK293 cells. HEK293 cells were treated with lung-cancer-derived EVs or transfected miR-103a mimics for 48 hr. The expression of proteins was assessed by immunoblot. (E and F) Ectopic expression of PTEN (E) prevents the effect of hypoxic CL1-5-derived EVs in M2 polarization (F). $CD14^{+}$ monocytes were transfected either with pCMV or PTEN cDNA and then treated with lung-cancer-derived EVs. The expression of surface markers was assessed by flow cytometry. Data are expressed as mean ± SD. *$p < 0.05$ between two groups. All experiments were performed independently at least 3 times. WT, wild-type; MT, mutated.

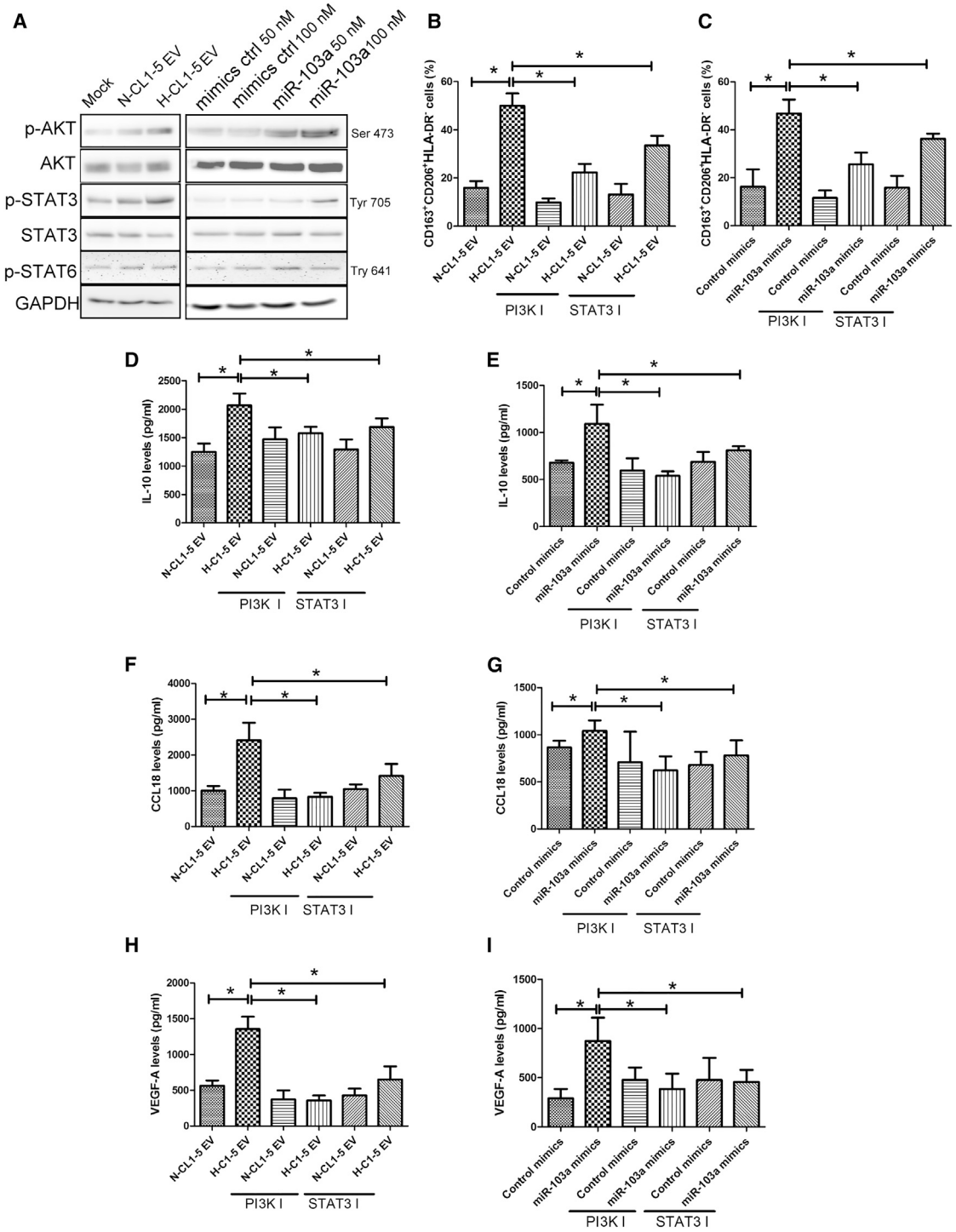

Figure 5. Activation of AKT, and STAT3 Is Involved in EV miR-103a-Mediated M2 Polarization

(A) Hypoxic CL1-5-derived EV miR-103a and miR-103a mimics increased the phosphorylation of AKT and STAT3. Cells were treated with lung-cancer-derived EVs or transfected miR-103a mimics for 48 hr. The expression of various proteins was assessed by immunoblot. (B–I) PI3K and STAT3 inhibitors decreased M2 polarization (B and C), IL-10 expression (D and E), CCL18 expression (F and G), and VEGF-A expression (H and I) induced by hypoxic CL1-5-derived EV miR-103a and miR-103a mimics. $CD14^+$ monocytes were treated with lung-cancer-derived EVs containing control vehicle, PI3K, or STAT3 inhibitors for 5 days. The expression of surface markers was assessed by flow cytometry, and the expression of secreted proteins was determined using the Luminex system. Data are expressed as means ± SD. *$p < 0.05$ between two groups. All experiments were performed independently at least 3 times. I, inhibitor.

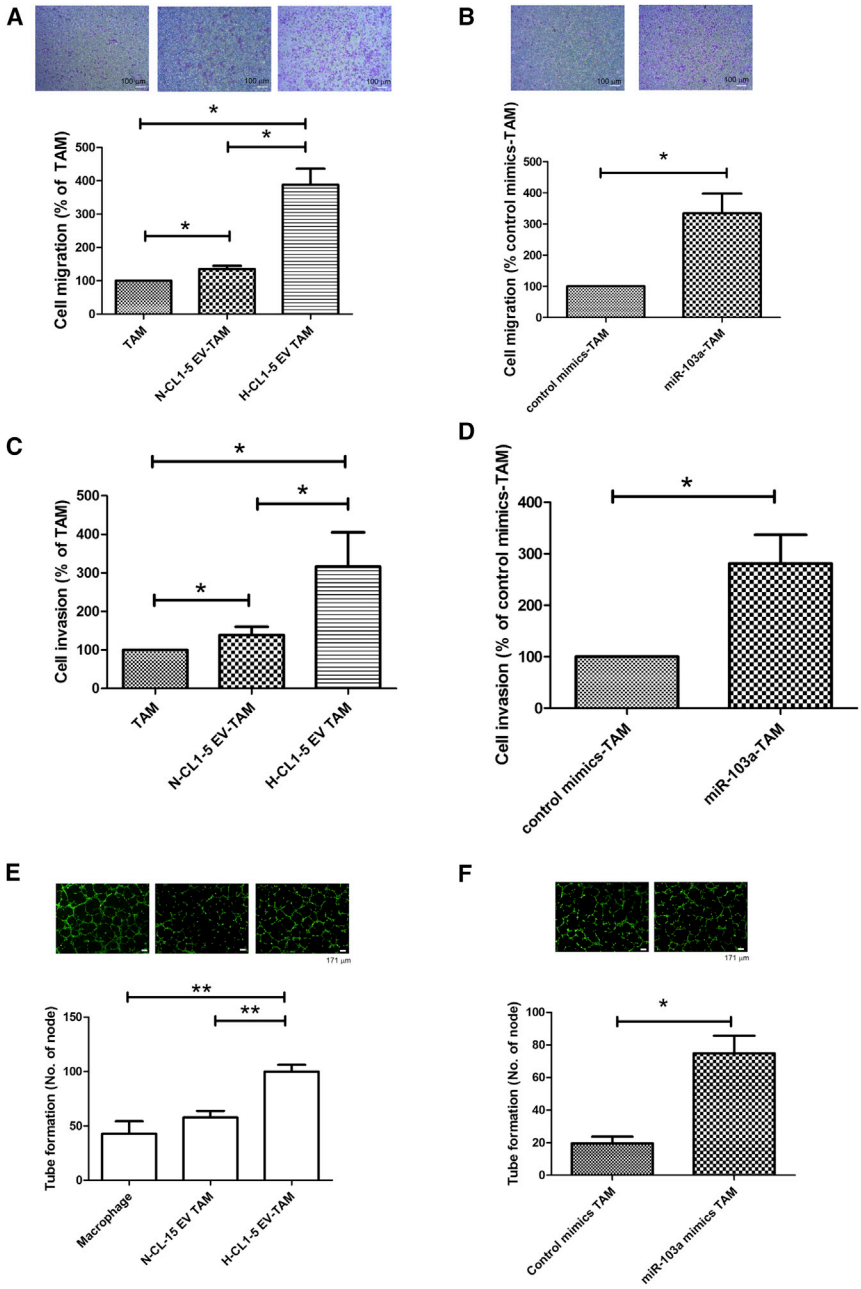

Figure 6. miR-103a-Conditioned Macrophages Increased Lung Cancer Migration and Angiogenesis

(A and B) Conditioned medium (CM) of macrophages derived from hypoxic CL1-5-derived EV miR-103a (A) and miR-103a mimics (B) increased CL1-5 migration. (C and D) Conditioned medium (CM) of macrophages derived from hypoxic CL1-5-derived EV miR-103a (C) and miR-103a mimics (D) increased CL1-5 invasion. (E and F) The CM of macrophages derived from hypoxic CL1-5-derived EV miR-103a (E) and miR-103a mimics (F) enhanced tube formation of HUVEC. $CD14^+$ monocytes were treated with lung-cancer-derived EVs or transfected with either control or miR-103a mimics and then cultured for another 5 days. CMs of various macrophages were collected and stored at −80°C. The migration of CL1-5 cells was assessed using a transwell assay. Tube formation of HUVECs was determined using Matrigel-coated methods. Data are expressed as means ± SD. *$p < 0.05$ between two groups. All experiments were performed independently at least 3 times. TAM, tumor-associated macrophage. Scale bar, 100 μm (A and B) and 171 μm (E and F).

(Lonza, Basel, Switzerland) supplemented with 10% fetal bovine serum (FBS), 100 U/mL penicillin, and 100 μg/mL streptomycin (Invitrogen, Carlsbad, CA, USA). HEK293 was cultured in Eagle's minimum essential medium with 10% FBS, 100 U/mL penicillin and 100 μg/mL streptomycin (Invitrogen, Carlsbad, CA). To obtain CL1-5-conditioned media (CM), the cells were seeded as 1×10^6 cells/100-mm dish and cultivated in normoxic or hypoxic conditions for 24 hr, and the supernatants (CM) were harvested after 24 hr of incubation. Pharmacological inhibitors AG490 and LY294002 (Calbiochem, Nottingham, UK) were used at a concentration (1 μM) that did not affect cell viability of macrophages. WST-1 was used to assess cancer cell viability. All cells tested negative for mycoplasma contamination using the MycoAlert Mycoplasma Detection Kit (Lonza) and were authenticated by short tandem repeats (Promega).

EV Isolation and Uptake

Lung cancer cells were cultured in 1% oxygen (hypoxic conditions) or 20% oxygen (normoxic conditions) in exosome-depleted medium (Invitrogen, Carlsbad, CA, USA) for 24 hr. EVs were isolated from the supernatants of normoxic and hypoxic lung cancer cells using exosome isolation kits (Invitrogen) after removing cell debris. The EVs were dissolved with PBS and stored at −80°C. The protein content of EVs was determined using a bicinchoninic acid (BCA) protein assay kit (Millipore, Billerica, MA, USA). Purified EVs were identified by immunblot for CD63, CD81, CD9, and HSP70,[24] and the number of EVs isolated from lung cancer cell lines was determined by an Exo-ELISA Kit (cat# EXOEL) (System Biosciences, Mountain View, CA, USA), which enables quantitation of characterized exosome markers: CD9, CD63, or CD81. The depletion of EVs from CM of normoxic and hypoxic CL1-5 cells was carried out by a microfiltration ExoMir PLUS Kit (Bioo Scientific, Austin, TX, USA).

Macrophage Generation and Cytokine Measurement

All blood samples were admitted to the Division of Pulmonary and Critical Care Medicine at Kaohsiung Medical University Hospital (KMUH), Kaohsiung, Taiwan. Serum was separated by centrifugation

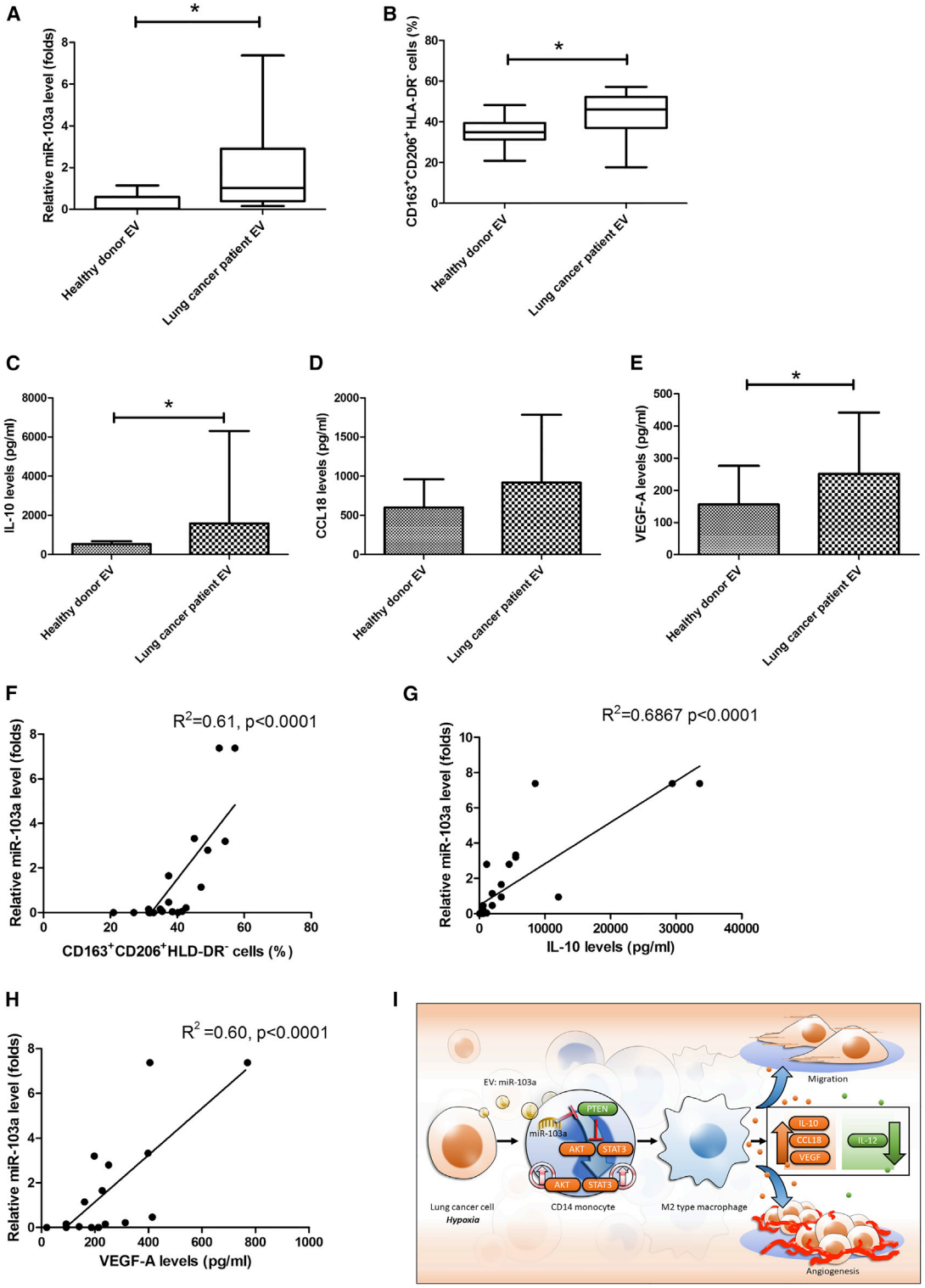

Figure 7. Levels of miR-103a in the Sera of Patients with Lung Cancer Are Correlated with the Activity of M2 Polarization

(A) Levels of EV miR-103a in patients with lung cancer. (B–E) EVs isolated from patients with lung cancer increased the population of $CD163^{+}CD206^{high}HLA\text{-}DR^{low}$ cells (B), IL-10 expression (C), CCL18 expression (D), and VEGF-A expression (E). (F–H) Positive correlation between EV miR-103a and M2 surface markers (F), IL-10 levels (G), and

(legend continued on next page)

and frozen at −80°C. The Institutional Review Board (IRB) of KMUH approved the study's protocol, and all participants provided written informed consent in accordance with the Declaration of Helsinkii. Peripheral blood mononuclear cells (PBMCs) from 10 different donors were isolated by centrifugation over a Ficoll gradient (GE Healthcare, Freiburg, Germany). $CD14^+$ cells were isolated from PBMCs with MACS technology using anti-$CD14^+$ microbeads (Miltenyi Biotec, Cologne, Germany).

Macrophage differentiation was performed to obtain M1 and M2 macrophages, and $CD14^+$ monocytes were cultured in RPMI1640 (Lonza, Basel, Switzerland) supplemented with 10% FBS (GIBCO, Grand Island, NY, USA) (control, ctr), with macrophage colony-stimulating factor (M-CSF) (20 ng/mL) (R&D Systems, Minneapolis, MN, USA) for 5 days, with replacement of half of the culture media at day 3. To assess the effect of lung-cancer-derived EVs, the same differentiation protocol was performed in the presence of EVs isolated from lung cancer cells under either normoxic or hypoxic conditions. The interaction of cancer cells with $CD14^+$ monocytes in a fixed ratio of monocytes/lung cancer cell (1:10). Equal amounts (1 μg EVs ≈ 4.5×10^6 EVs) of normoxic or hypoxic CL1-5-derived EV, as determined by BCA quantitation, were used in every independent experiment. For inhibition experiments, PI3K and STAT3 inhibitors were pre-added for 2 hr at a concentration of 1 μM. The various cytokine levels were determined by Luminex Assays (R&D Systems). Macrophage supernatants were collected, centrifuged for 10 mn at 3,000 × *g*, and stored at −80°C until further analysis or use as a conditioned medium (CM).

Flow Cytometry

To analyze surface markers, cells were stained with primary antibody against a specific antigen or corresponding isotype control antibodies in PBS containing 2% (w/v) bovine serum albumin. The following antibodies were used: phycoerythrin (PE)-labeled anti-CD80 and anti-CD163 antibody, fluorescein isothiocyanate (FITC)-labeled anti-human leukocyte antigen (HLA)-DR or anti-CD14 antibody, and allophycocyanin (APC)-labeled anti-CD206 antibody. All primary and isotype antibodies were obtained from BD Biosciences. Flow cytometric data were acquired by Accuri C6 flow cytometer (BD Biosciences) and analyzed using CellQuest software (BD Biosciences).

Quantitative Real-Time PCR

Total RNA was extracted from cultured cells and EVs using TRIzol and TRIzolLS Reagents (Life Technologies). cDNA was prepared using an oligo (dT) primer and reverse transcriptase (Takara, Shiga, Japan) following standard protocols. miRNAs were reverse transcribed using the Mir-X miRNA First Strand Synthesis Kit (Clontec). mRNA levels were performed using real-time analysis with SYBR Green on a StepOne-Plus machine (Applied Biosystems, Foster City, CA, USA). The relative expression levels of the cellular mRNA and miRNA were normalized to glyceraldehyde 3-phosphate dehydrogenase or U6 small nuclear RNA (snRNA), respectively. EV miRNA purified from serum was normalized with cel-miR-39 (Exiqon, Vedbaek, Denmark) as a spike-in control, and compared with a reference sample. The primers used are listed in Table S2. The relative standard curve method ($2^{-\Delta\Delta Ct}$) was used to determine relative mRNA or miRNA expression.

MicroRNA Mimics, Inhibitor, siRNA Transfection, and PTEN Overexpression

HEK293, $CD14^+$ monocytes, or macrophages were transfected with control mimics, an miR-103a mimic (50 or 100 nM), a control inhibitor, or an miR-103a inhibitor (100 nM) using Dharmafect reagents (number 1 for HEK239 cells and number 3 for monocytes and macrophages) (Dharmacon, Lafayette, CO, USA). Oligonucleotides with random sequences served as negative controls for an miRNA mimic or an inhibitor (Dharmacon). For PTEN knockdown, $CD14^+$ monocytes or macrophages were transfected with ONTARGET plus control siRNA or PTEN siRNA (Dharmacon), in accordance with the manufacturer's protocol. Cells were harvested 48 or 72 hr post-transfection for mRNA and protein analyses. Overexpression of PTEN was achieved by transfecting PTEN cDNA (Origene Technologies, Rockville, MD, USA) via Turbofect transfection (Thermo Fisher, Boston, MA, USA).

Detection of miR-103a Transfer *In Vitro*

CL1-5 cells were transfected with naked or Cy5-labeled miR-103a oligo (Dharmacon) for 24 hr. Cells were washed with PBS and incubated with RPMI1640 medium containing exosome-free FBS for 24 hr. EVs were isolated from the conditioned medium by the procedure described above and then added to Calcein AM-labeled $CD14^+$ monocytes. EV uptake by monocytes was imaged using an inverted Nikon Eclipse TE300 microscope (Nikon).

3′ UTR Luciferase Reporter Analysis

HEK293 cells were transfected with 0.4 μg of the PTEN reporter plasmid containing the predicted miR-103a-binding sites (Addgene, plasmid 21326) or mutated miR-103a-binding sites/Renilla luciferase plasmid (Promega, Madison, WI) (10:1), together with control mimics or miR-103a mimics, using a DharmaFECT duo transfection reagent (Dharmacon) in accordance with the manufacturer's protocol. The cells were washed, and luciferase activity was determined by a Dual-Luciferase Reporter Assay System (Promega). Relative luciferase activity was first normalized by Renilla luciferase activity and then compared with those of the respective controls.

Immunoblot

Cell extracts were prepared using ice-cold RIPA lysis buffer (EMD Millipore, Billerica, MA, USA) containing a protease inhibitor

VEGF-A expression (H). (I) Model for how hypoxic lung-cancer-derived EVs increase M2 polarization of macrophages, which in turn enhance cancer progression and angiogenesis. $CD14^+$ monocytes were treated with EVs (10 μg) isolated from the sera of healthy donors or patients with lung cancer, which contained M-CSF, for 5 days. The expression of surface markers was assessed by flow cytometry, and the expression of secreted proteins was determined by the Luminex system. Data are expressed as mean ± SD. *$p < 0.05$.

cocktail (Sigma, St. Louis, MO, USA). The protein extracts were denatured in a boiling water bath for 5 min and then resolved by SDS-PAGE. Proteins were transferred to polyvinylidene fluoride (PVDF) membranes (EMD Millipore), which were probed with primary antibodies overnight at 4°C, followed by incubation with horseradish peroxidase (HRP)-conjugated secondary antibodies at 1:4,000 dilutions (Cell-Signaling Technology, Danvers, MA, USA) for 1 hr at room temperature. The signal of the targeted protein was developed using a chemiluminescence kit (EMD Millipore). Primary antibodies used include those against PTEN (catalog no. 9188), p-AKT (catalog no. 4060), AKT (catalog no. 4691), p-STAT3 (catalog no. 9131), STAT3 (catalog no. 4904), p-STAT6 (catalog no. 9361), STAT6 (catalog no. 9362) (Cell-Signaling Technology, Danvers, MA, USA), and GAPDH (EMD Millipore, catalog no. MAB374). To quantify the immunoblot images on unsaturated bands, densitometric analysis was performed using AlphaEaseFC (Alpha Innotech) followed by statistical evaluation.

Cell Migration and Endothelial Cell Tube Formation Assay

Human umbilical vein endothelial cells (HUVECs) (8×10^4 cells/well) were seeded onto growth-factor-reduced BD Matrigel (1 mg/mL) (BD Biosciences) for 1 hr. Cells were supplemented for the CMs of macrophages, which were treated with normoxic CL1-5 or hypoxic CL1-5-derived EVs or transfected with control mimics or mR-103a mimics. HUVECs were stained by Calcein AM (Invitrogene) for 30 min and imaged using an inverted Nikon Eclipse TE300 microscope (Nikon).

Statistical Analysis

Data are expressed as means ± SD. Multiple group comparisons were performed by two-way analysis of variance (one-way ANOVA) with Tukey's post hoc test, which was used with the assistance of the GraphPad Prism program (Graphpad Software, San Diego, CA, USA). Two treatment groups were compared using a Student's t test. Results are considered statistically significant when $p < 0.05$.

SUPPLEMENTAL INFORMATION

Supplemental Information includes four figures and two tables and can be found with this article online at https://doi.org/10.1016/j.ymthe.2017.11.016.

AUTHOR CONTRIBUTIONS

Y.-L.H. and P.-L.K. designed the study, analyzed the data, and wrote the manuscript. J.-Y.H. and W.-A.C. collected the clinical samples and analyzed the clinical data. S.-F.J., Y.-S.L., and Y.-C.P. participated in the experiment and performed data analysis. Y.-C.P. and C.-Y.W. performed the animal experiments. All authors read and approved the final manuscript.

CONFLICTS OF INTEREST

We declare that we have no conflicts of interest.

ACKNOWLEDGMENTS

This study was supported by grants from the Ministry of Science and Technology (MOST) (104-2314-B-037-053-MY4; 104-2320-B-037-014-MY3), Kaohsiung Medical University Hospital (KMUHS10601), and the "KMU-KMUH Co-Project of Key Research" (KMU-DK 107009 from Kaohsiung Medical University).

REFERENCES

1. Didkowska, J., Wojciechowska, U., Mańczuk, M., and Łobaszewski, J. (2016). Lung cancer epidemiology: contemporary and future challenges worldwide. Ann. Transl. Med. *4*, 150.
2. Dizon, D.S., Krilov, L., Cohen, E., Gangadhar, T., Ganz, P.A., Hensing, T.A., Hunger, S., Krishnamurthi, S.S., Lassman, A.B., Markham, M.J., et al. (2016). Clinical cancer advances 2016: annual report on progress against cancer from the American Society of Clinical Oncology. J. Clin. Oncol. *34*, 987–1011.
3. Siegel, R.L., Miller, K.D., and Jemal, A. (2015). Cancer statistics, 2015. CA Cancer J. Clin. *65*, 5–29.
4. Ugel, S., De Sanctis, F., Mandruzzato, S., and Bronte, V. (2015). Tumor-induced myeloid deviation: when myeloid-derived suppressor cells meet tumor-associated macrophages. J. Clin. Invest. *125*, 3365–3376.
5. Quatromoni, J.G., and Eruslanov, E. (2012). Tumor-associated macrophages: function, phenotype, and link to prognosis in human lung cancer. Am. J. Transl. Res. *4*, 376–389.
6. Zhang, B., Yao, G., Zhang, Y., Gao, J., Yang, B., Rao, Z., and Gao, J. (2011). M2-polarized tumor-associated macrophages are associated with poor prognoses resulting from accelerated lymphangiogenesis in lung adenocarcinoma. Clinics (São Paulo) *66*, 1879–1886.
7. Ding, T., Xu, J., Wang, F., Shi, M., Zhang, Y., Li, S.P., and Zheng, L. (2009). High tumor-infiltrating macrophage density predicts poor prognosis in patients with primary hepatocellular carcinoma after resection. Hum. Pathol. *40*, 381–389.
8. De Palma, M., and Lewis, C.E. (2013). Macrophage regulation of tumor responses to anticancer therapies. Cancer Cell *23*, 277–286.
9. Singh, S., Mehta, N., Lilan, J., Budhthoki, M.B., Chao, F., and Yong, L. (2017). Initiative action of tumor-associated macrophage during tumor metastasis. Biochimie *4*, 8–18.
10. Murray, P.J., Allen, J.E., Biswas, S.K., Fisher, E.A., Gilroy, D.W., Goerdt, S., Gordon, S., Hamilton, J.A., Ivashkiv, L.B., Lawrence, T., et al. (2014). Macrophage activation and polarization: nomenclature and experimental guidelines. Immunity *41*, 14–20.
11. Su, S., Liu, Q., Chen, J., Chen, J., Chen, F., He, C., Huang, D., Wu, W., Lin, L., Huang, W., et al. (2014). A positive feedback loop between mesenchymal-like cancer cells and macrophages is essential to breast cancer metastasis. Cancer Cell *25*, 605–620.
12. Belmont, L., Rabbe, N., Antoine, M., Cathelin, D., Guignabert, C., Kurie, J., Cadranel, J., and Wislez, M. (2014). Expression of TLR9 in tumor-infiltrating mononuclear cells enhances angiogenesis and is associated with a worse survival in lung cancer. Int. J. Cancer *134*, 765–777.
13. Conway, E.M., Pikor, L.A., Kung, S.H.Y., Hamilton, M.J., Lam, S., Lam, W.L., and Bennewith, K.L. (2016). Macrophages, inflammation, and lung cancer. Am. J. Respir. Crit. Care Med. *193*, 116–130.
14. Chen, Y.C.E., Mapp, S., Blumenthal, A., Burgess, M.L., Mazzieri, R., Mattarollo, S.R., Mollee, P., Gill, D., and Saunders, N.A. (2017). The duality of macrophage function in chronic lymphocytic leukaemia. Biochim. Biophys. Acta *1868*, 176–182.
15. Qian, B.Z., and Pollard, J.W. (2010). Macrophage diversity enhances tumor progression and metastasis. Cell *141*, 39–51.
16. Casazza, A., Laoui, D., Wenes, M., Rizzolio, S., Bassani, N., Mambretti, M., Deschoemaeker, S., Van Ginderachter, J.A., Tamagnone, L., and Mazzone, M. (2013). Impeding macrophage entry into hypoxic tumor areas by Sema3A/Nrp1 signaling blockade inhibits angiogenesis and restores antitumor immunity. Cancer Cell *24*, 695–709.
17. Becker, A., Thakur, B.K., Weiss, J.M., Kim, H.S., Peinado, H., and Lyden, D. (2016). Extracellular vesicles in cancer: cell-to-cell mediators of metastasis. Cancer Cell *30*, 836–848.
18. Pitt, J.M., Kroemer, G., and Zitvogel, L. (2016). Extracellular vesicles: masters of intercellular communication and potential clinical interventions. J. Clin. Invest. *126*, 1139–1143.

19. Yang, Q., Diamond, M.P., and Al-Hendy, A. (2016). The emerging role of extracellular vesicle-derived miRNAs: implication in cancer progression and stem cell related diseases. J. Clin. Epigenet. *2*, 13.

20. Triner, D., and Shah, Y.M. (2016). Hypoxia-inducible factors: a central link between inflammation and cancer. J. Clin. Invest. *126*, 3689–3698.

21. Rankin, E.B., and Giaccia, A.J. (2016). Hypoxic control of metastasis. Science *352*, 175–180.

22. Labiano, S., Palazon, A., and Melero, I. (2015). Immune response regulation in the tumor microenvironment by hypoxia. Semin. Oncol. *42*, 378–386.

23. Henze, A.T., and Mazzone, M. (2016). The impact of hypoxia on tumor-associated macrophages. J. Clin. Invest. *126*, 3672–3679.

24. Hsu, Y.L., Hung, J.Y., Chang, W.A., Lin, Y.S., Pan, Y.C., Tsai, P.H., Wu, C.Y., and Kuo, P.L. (2017). Hypoxic lung cancer-secreted exosomal miR-23a increased angiogenesis and vascular permeability by targeting prolyl hydroxylase and tight junction protein ZO-1. Oncogene *36*, 4929–4942.

25. Li, N., Qin, J., Lan, L., Zhang, H., Liu, F., Wu, Z., Ni, H., and Wang, Y. (2015). PTEN inhibits macrophage polarization from M1 to M2 through CCL2 and VEGF-A reduction and NHERF-1 synergism. Cancer Biol. Ther. *16*, 297–306.

26. Yue, S., Rao, J., Zhu, J., Busuttil, R.W., Kupiec-Weglinski, J.W., Lu, L., Wang, X., and Zhai, Y. (2014). Myeloid PTEN deficiency protects livers from ischemia reperfusion injury by facilitating M2 macrophage differentiation. J. Immunol. *192*, 5343–5353.

27. Noy, R., and Pollard, J.W. (2014). Tumor-associated macrophages: from mechanisms to therapy. Immunity *41*, 49–61.

28. Casazza, A., Di Conza, G., Wenes, M., Finisguerra, V., Deschoemaeker, S., and Mazzone, M. (2014). Tumor stroma: a complexity dictated by the hypoxic tumor microenvironment. Oncogene *33*, 1743–1754.

29. Liu, Y., Gu, Y., Han, Y., Zhang, Q., Jiang, Z., Zhang, X., Huang, B., Xu, X., Zheng, J., and Cao, X. (2016). Tumor exosomal RNAs promote lung pre-metastatic niche formation by activating alveolar epithelial TLR3 to recruit neutrophils. Cancer Cell *30*, 243–256.

30. Zhao, L., Liu, W., Xiao, J., and Cao, B. (2015). The role of exosomes and "exosomal shuttle microRNA" in tumorigenesis and drug resistance. Cancer Lett. *356* (2 Pt B), 339–346.

31. Qu, L., Ding, J., Chen, C., Wu, Z.J., Liu, B., Gao, Y., Chen, W., Liu, F., Sun, W., Li, X.F., et al. (2016). Exosome-transmitted lncARSR promotes sunitinib resistance in renal cancer by acting as a competing endogenous RNA. Cancer Cell *29*, 653–668.

32. Weber, D.G., Johnen, G., Bryk, O., Jöckel, K.H., and Brüning, T. (2012). Identification of miRNA-103 in the cellular fraction of human peripheral blood as a potential biomarker for malignant mesothelioma–a pilot study. PLoS ONE *7*, e30221.

33. Xia, W., Ni, J., Zhuang, J., Qian, L., Wang, P., and Wang, J. (2016). MiR-103 regulates hepatocellular carcinoma growth by targeting AKAP12. Int. J. Biochem. Cell Biol. *71*, 1–11.

34. Zheng, Y.B., Xiao, K., Xiao, G.C., Tong, S.L., Ding, Y., Wang, Q.S., Li, S.B., and Hao, Z.N. (2016). MicroRNA-103 promotes tumor growth and metastasis in colorectal cancer by directly targeting LATS2. Oncol. Lett. *12*, 2194–2200.

35. Akers, J.C., Ramakrishnan, V., Kim, R., Phillips, S., Kaimal, V., Mao, Y., Hua, W., Yang, I., Fu, C.C., Nolan, J., et al. (2015). miRNA contents of cerebrospinal fluid extracellular vesicles in glioblastoma patients. J. Neurooncol. *123*, 205–216.

36. Chen, Z., Lai, T.C., Jan, Y.H., Lin, F.M., Wang, W.C., Xiao, H., Wang, Y.T., Sun, W., Cui, X., Li, Y.S., et al. (2013). Hypoxia-responsive miRNAs target argonaute 1 to promote angiogenesis. J. Clin. Invest. *123*, 1057–1067.

37. Xiao, J., Hu, C.P., He, B.X., Chen, X., Lu, X.X., Xie, M.X., Li, W., He, S.Y., You, S.J., and Chen, Q. (2016). PTEN expression is a prognostic marker for patients with non-small cell lung cancer: a systematic review and meta-analysis of the literature. Oncotarget *7*, 57832–57840.

38. Bronisz, A., Godlewski, J., Wallace, J.A., Merchant, A.S., Nowicki, M.O., Mathsyaraja, H., Srinivasan, R., Trimboli, A.J., Martin, C.K., Li, F., et al. (2011). Reprogramming of the tumour microenvironment by stromal PTEN-regulated miR-320. Nat. Cell Biol. *14*, 159–167.

39. Trimboli, A.J., Cantemir-Stone, C.Z., Li, F., Wallace, J.A., Merchant, A., Creasap, N., Thompson, J.C., Caserta, E., Wang, H., Chong, J.L., et al. (2009). Pten in stromal fibroblasts suppresses mammary epithelial tumours. Nature *461*, 1084–1091.

40. Sahin, E., Haubenwallner, S., Kuttke, M., Kollmann, I., Halfmann, A., Dohnal, A.M., Chen, L., Cheng, P., Hoesel, B., Einwallner, E., et al. (2014). Macrophage PTEN regulates expression and secretion of arginase I modulating innate and adaptive immune responses. J. Immunol. *193*, 1717–1727.

41. Wang, G., Shi, Y., Jiang, X., Leak, R.K., Hu, X., Wu, Y., Pu, H., Li, W.W., Tang, B., Wang, Y., et al. (2015). HDAC inhibition prevents white matter injury by modulating microglia/macrophage polarization through the GSK3β/PTEN/Akt axis. Proc. Natl. Acad. Sci. USA *112*, 2853–2858.

YMTHE, Volume *26*

Supplemental Information

Hypoxic Lung-Cancer-Derived Extracellular Vesicle MicroRNA-103a Increases the Oncogenic Effects of Macrophages by Targeting PTEN

Ya-Ling Hsu, Jen-Yu Hung, Wei-An Chang, Shu-Fang Jian, Yi-Shiuan Lin, Yi-Chung Pan, Cheng-Ying Wu, and Po-Lin Kuo

sTable 1. Four hypoxic lung cancer cell lines-secreted exosomes increased the expression of M2 type cytokines and proangiogenic factors.

	H-1437		H-1792		H-2087	
	Normoxia	**Hypoxia**	**Normoxia**	**Hypoxia**	**Normoxia**	**Hypoxia**
Cytokines (pg/ml)						
IL-12	4.25± 6.62	5.13±9.15	1.05±0.72	2.43±2.33	4.99±1.58	11.31±14.89
IL-10	713.6469±111.22	1025.57*±272.10	498.21±154.32	1141.51*±403.82	686.311±206.14	1275.68*±635.03
CCL18	851.11±37.511	1019.91*±316.95	1165.46±323.88	2550.43*±251.89	1038.26±326.74	1516.96*±408.89
CCL22	706.83±255.18	1605.43*±460.17	2499.67±820.60	3471.553*±308.47	1287.51±133.23	2677.45*±799.47
TNF-α	927.02±159.43	1441.47±342.14	366.65±140.99	635.70*±190.69	754.41±124.20	1375.73*±285.09
Proangiogenic factors (pg/ml)						
VEGF-A	98.35±140.46	355.72*±128.88	270.93±38.85	932.51*±135.71	115.73±120.20	266.77*±23.54
Angiopoietin-1	406.87±87.44	785.58*±64.90	396.43±170.40	870.42*±104.43	450.79±47.04	748.38*±73.46
Angiogenin	1796.62±737.99	2048.46±943.37	544.65±165.89	1080.58±388.00	904.81±302.81	1720.78±638.70
FGF basic	5.86±1.93	8.63±0.835	9.23±3.72	12.39±12.92	5.44±1.02	10.41±5.02
FGF acidic	3.14±0.69	3.37±0.63	3.31±0.42	3.27±1.03	3.32±0.59	4.67±5.01
PDGF-AA	11.27±7.12	18.00±4.22	24.33±11.32	27.00±18.50	13.70±2.22	12.83±6.19
PDGF-BB	304.31±89.72	436.54±35.50	176.07±68.48	199.02±63.31	305.08±25.88	311.41±30.34
PIGF	0.68±0.18	0.97±0.27	0.98±0.04	1.08±0.26	0.97±0.06	0.74±0.98
VEGF-D	13.23956±0.51	13.16±2.10	12.42±2.43	11.60±0.81	11.02±0.72	16.32±6.16

*, $p<0.05$ vs. Normoxia

sTable 2. The sequence of primers

miRNA	Primer sequence
has-miR-103a-5p	5'AGCTTCTTTACAGTGCTGCCTTG 3'
has-miR-103a-3p	5'AGCAGCATTGTACAGGGCTATGA 3'
pre-miR-103a	left: 5′CCCTCGGCTTCTTTACAGTG3′; right: 5′CAATGCCTTCATAGCCCTG3′
U6	left: TGGAACGCTTCACGAATTTGCG; right: GGAACGATACAGAGAAGATTAGC
PTEN	left: CGACGGGAAGACAAGTTCAT right: AGGTTTCCTCTGGTCCTGGT
GAPDH	left: GAGTCAACGGATTTGGTCGT; right: TTGATTTTGGAGGGATCTCG

sFigure Legends

sFigure 1. Depletion of EVs reduced M2 polarization induced by hypoxic CL1-5 cells. Removal of EVs from condition medium of hypoxic CL1-5 medium decreased M2 polarization (A), IL-10 (B) ,CCL18 (C), and CCL22 (D) production. The EVs of CL1-5 condition medium were removed by microfiltration ExoMir™ PLUS Kit. $CD14^+$ monocytes (1×10^5 cells) were treated with EVs-depletion or non-depletion condition medium collected from normoxic (20% oxygen, 24 h culture, 1×10^6 cells) and hypoxic CL-15 cells (1% oxygen, 24 h culture, 1×10^6 cells), which contained M-CSF (20 ng/ml), for 5 days. Various surface marker expressions were stained, then assessed by flow cytometry. The expression of secreted proteins was determined by the Luminex system. Data are expressed as mean ± standard deviation (SD).* indicates P <0.05. All experiments were performed independently at least 3 times. CM, condition medium

sFigure 2. The level of miR-103a in lung cancer-derived EVs. (A) The levels of miR-103a in an equal number of EVs isolated from normoxic and hypoxic CL1-5 cells. The number of EVs isolated from normoxic and hypoxic EVs was determined by Exo-ELISA™ kits. (B) The levels of pri/pre miR-103a in EVs of normoxic and hypoxic CL1-5 cells. (C) The levels of miR-103a in EVs isolated from four lung cancer cell lines in both normoxic and hypoxic conditions. The level of pre/pri- and

mature miR-103a assessed by qRT-PCR. Data are expressed as mean ± standard deviation (SD).* indicates P <0.05; ns., not significant. All experiments were performed independently at least 3 times.

sFigure 3. Hypoxic CL1-5-derived EVs miR-103a and miR-103a decreased the expression of PTEN in monocytes. (A) Sequence alignment of miR-103 in the *PTEN* 3′ UTR in different species. (B) The effect of hypoxic CL1-5-derived EVs miR-103a and miR-103a in the expression of PTEN. CD14+ monocytes were treated with lung cancer-derived EVs or transfected miR-103a mimics for 48 h. The expression of proteins was assessed by immunoblot. All experiments were performed independently at least 3 times.

sFigure 4. Inhibition of PTEN increases M2 polarization and M2 type cytokine expression. (A) The knockdown efficacy of PTEN siRNA. (B) Flow cytometry analysis reveals that the transfection of PTEN siRNA increases the population of $CD163^{+}CD206^{high}HLA\text{-}DR^{low}$ cells. The effects of PTEN siRNA transfection on the expression of IL-10 (C), CCL18 (D) and VEGF-A (E). $CD14^{+}$ monocytes were transfected with either control or PTEN siRNA and then cultured for another 5 days. The level of PTEN was assessed by qRT-PCR. The expression of surface markers was assessed by flow cytometry and the expression of secreted proteins determined by the Luminex system. Data are expressed as mean ± standard deviation (SD).* indicates

P <0.05. All experiments were performed independently at least 3 times.

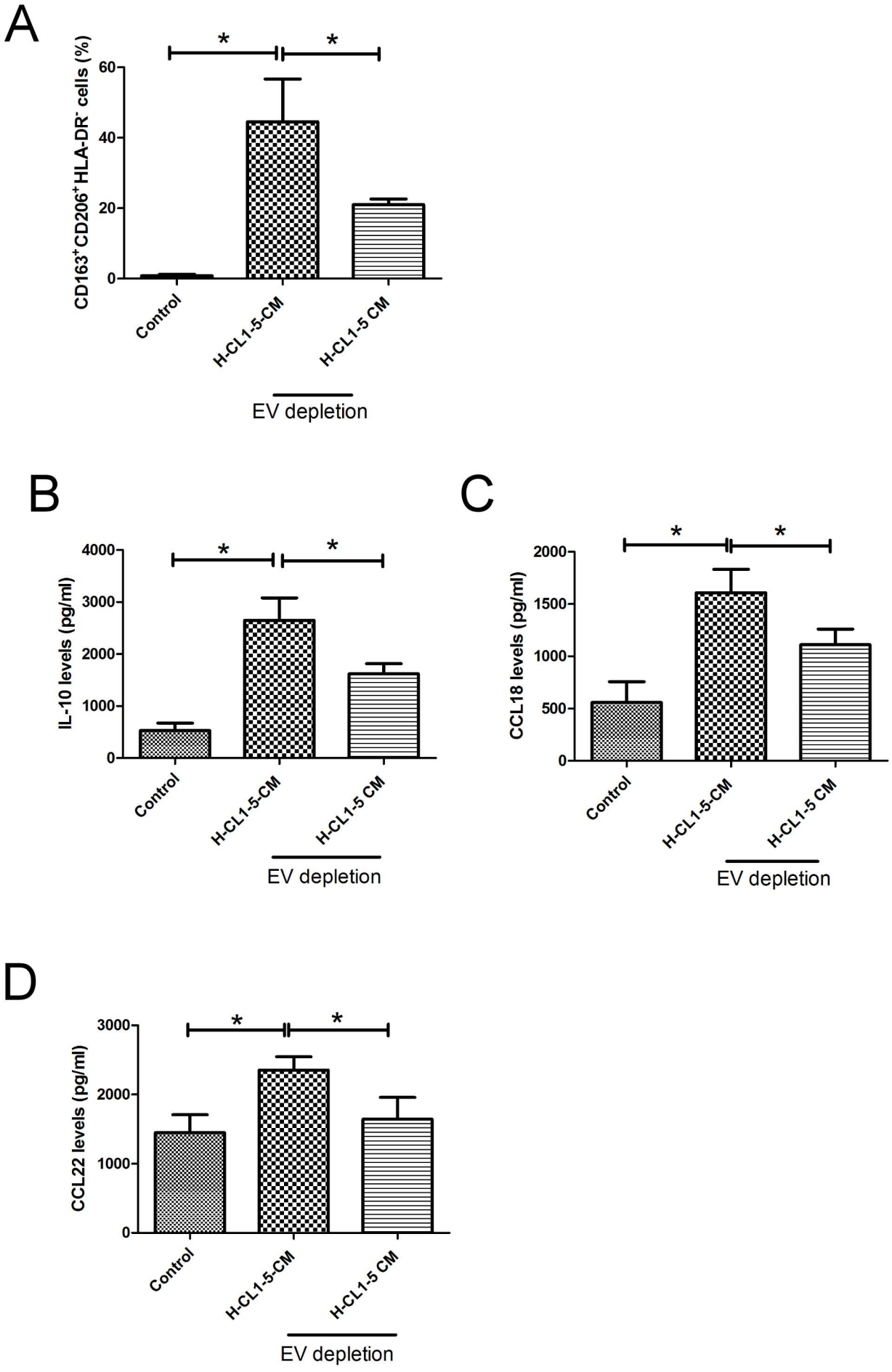
A
CD163+CD206+HLA-DR- cells (%)
60
40
20
0
*
*
Control
H-CL1-5-CM
H-CL1-5 CM
EV depletion
B
IL-10 levels (pg/ml)
4000
3000
2000
1000
0
*
*
Control
H-CL1-5-CM
H-CL1-5 CM
EV depletion
C
CCL18 levels (pg/ml)
2000
1500
1000
500
0
*
*
Control
H-CL1-5-CM
H-CL1-5 CM
EV depletion
D
CCL22 levels (pg/ml)
3000
2000
1000
0
*
*
Control
H-CL1-5-CM
H-CL1-5 CM
EV depletion

sFigure 1

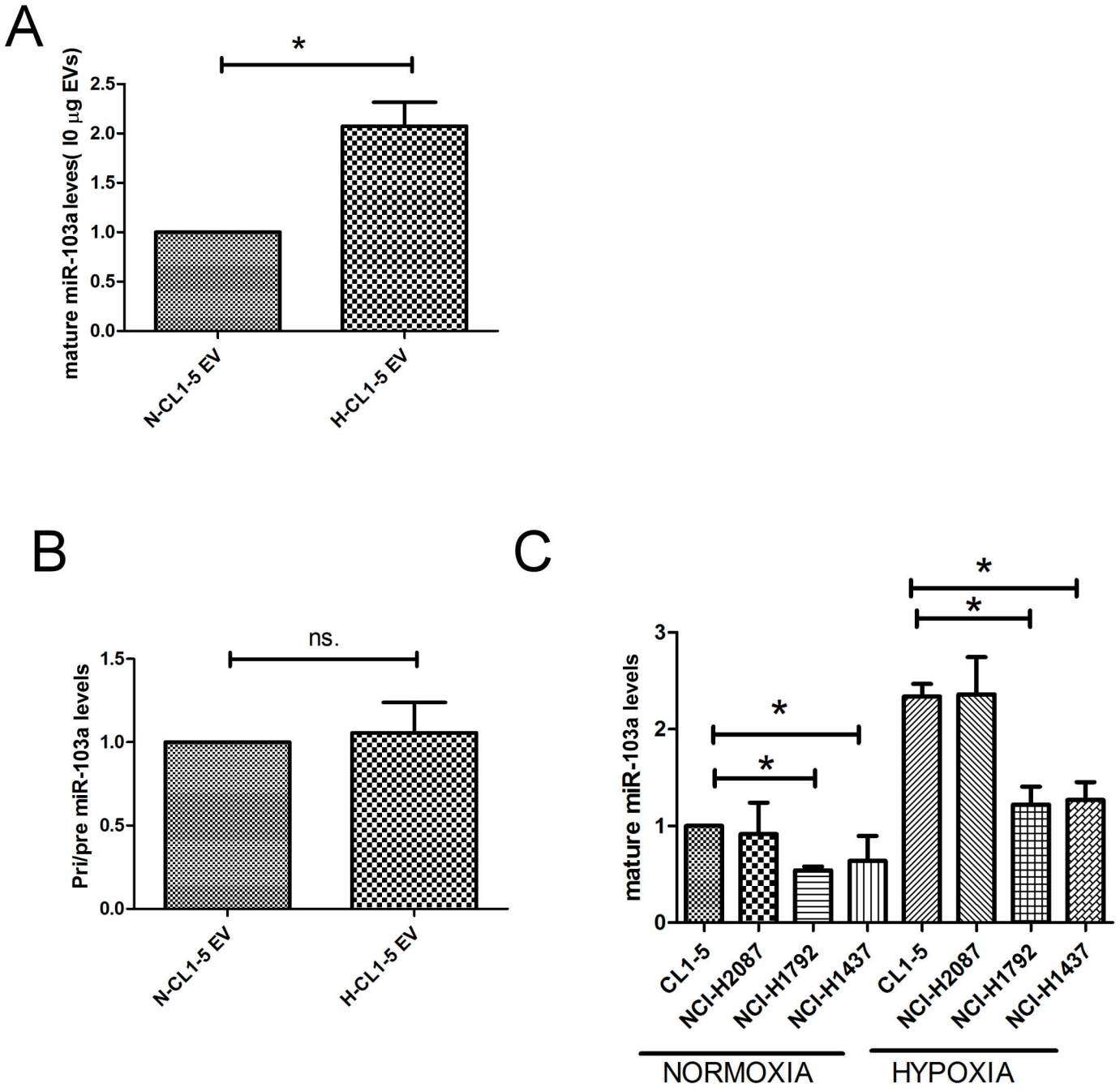
A
*
mature miR-103a leves(I0 μg EVs)
2.5
2.0
1.5
1.0
0.5
0.0
N-CL1-5 EV
H-CL1-5 EV
B
ns.
Pri/pre miR-103a levels
1.5
1.0
0.5
0.0
N-CL1-5 EV
H-CL1-5 EV
C
*
*
*
*
mature miR-103a levels
3
2
1
0
CL1-5
NCI-H2087
NCI-H1792
NCI-H1437
CL1-5
NCI-H2087
NCI-H1792
NCI-H1437
NORMOXIA
HYPOXIA

sFigure 2

A


Human --UUUGUAAUGCUGCACAGAAAUUU--
Chimp --UUUGUAAUGCUGCACAGAAAUUU--
Rhesus --UUUGUAAUGCUGCACAGAAAUUU--
Squirrel --UUUGUAAUGCUGCACAGAAAUUU--
Pig --UUUGUAAUGCUGCACAGAAAUUU--
Cow --UUUGUAAUGCUGCACAGAAAUUU--
CAT --UUUGUAAUGCUGCACAGAAAUUU--
Dog --UUUGUAAUGCUGCACAGAAAUUU--
Brown bat --UUUGUAAUGCUGCACAGAAAUUU--
Elephant --UUUGUAAUGCUGCACAGAAAUUU--
miR-103a-3p
AGUAUCGGGACAUGUUACGACGA

B

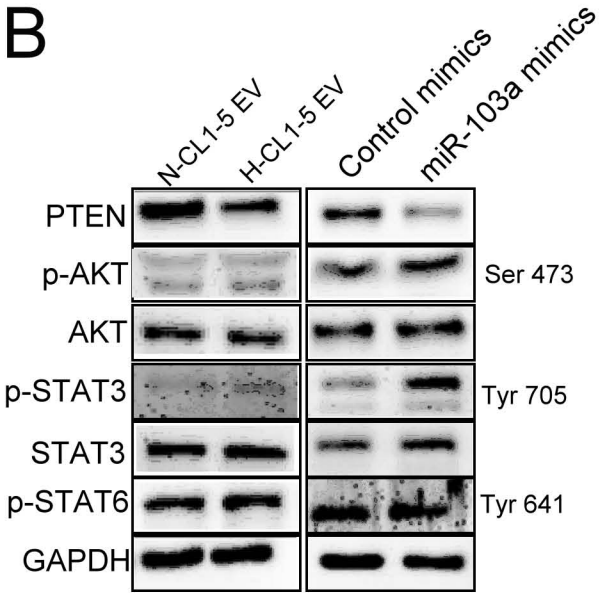
N-CL1-5 EV
H-CL1-5 EV
Control mimics
miR-103a mimics
PTEN
p-AKT
Ser 473
AKT
p-STAT3
Tyr 705
STAT3
p-STAT6
Tyr 641
GAPDH

sFigure 3

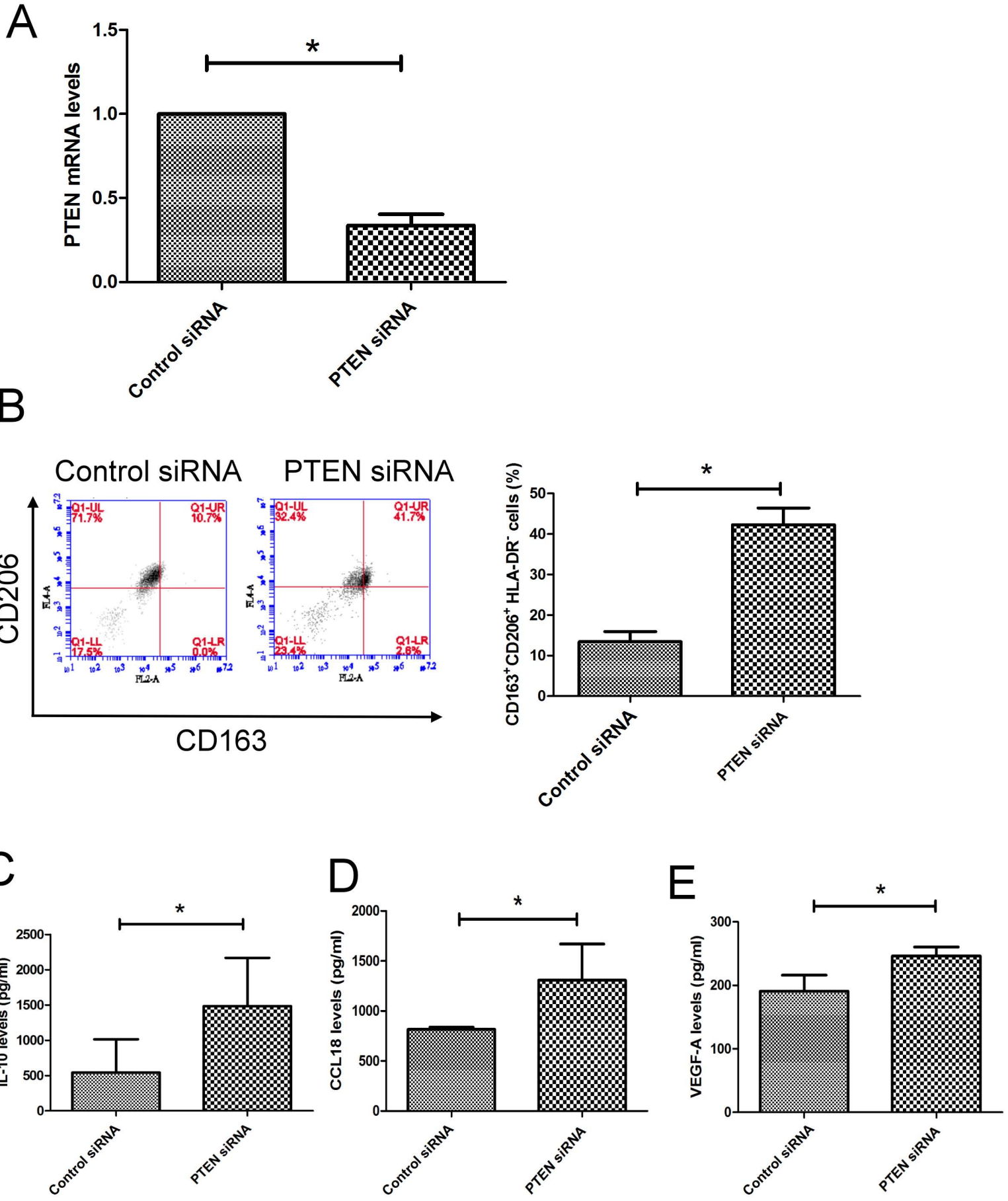
A
PTEN mRNA levels
1.5
1.0
0.5
0.0
*
Control siRNA
PTEN siRNA
B
Control siRNA
PTEN siRNA
CD206
CD163
Q1-UL 71.7%
Q1-UR 10.7%
Q1-LL 17.5%
Q1-LR 0.0%
Q1-UL 32.4%
Q1-UR 41.7%
Q1-LL 23.4%
Q1-LR 2.8%
FL4-A
FL2-A
CD163+CD206+ HLA-DR- cells (%)
50
40
30
20
10
0
*
Control siRNA
PTEN siRNA
C
IL-10 levels (pg/ml)
2500
2000
1500
1000
500
0
*
Control siRNA
PTEN siRNA
D
CCL18 levels (pg/ml)
2000
1500
1000
500
0
*
Control siRNA
PTEN siRNA
E
VEGF-A levels (pg/ml)
300
200
100
0
*
Control siRNA
PTEN siRNA

sFigure 4